# TRIP B3: LATE PROTEROZOIC SHEAR ZONES OF THE WESTERN HUDSON AND NEW JERSEY HIGHLANDS

MICHAEL J. KALCZYNSKI and ALEXANDER E. GATES
*Department of Earth & Environmental Sciences, Rutgers University, Newark, NJ 07102*

## ABSTRACT

Multiple phases of deformation associated with the Grenville orogeny are recorded in the rocks exposed in the northern Reading Prong of southeastern New York and northern New Jersey. The rocks of the Hudson and New Jersey Highlands are considered to have formed in an island arc or marine magmatic arc setting ca. ~1.3 Ga, as volcanics, volcaniclastics, and sedimentary rocks. Deposition terminated when continental collision resulted in the formation of a major mountain belt during the onset of the Grenville orogeny. Granulite facies metamorphism created the dominantly gneissic regional foliation and migmatization, with extensive pegmatite intrusion. During this time, the Ramapo and Reservoir faults were established as zones of major crustal weakness. Dioritic dike and stock intrusions occur shortly afterwards, but prior to the second event. The second Grenville deformational event was likely due to tectonic escape and resulted in the reactivation and creation of multiple dextral shear zones late in the Proterozoic.

The northeast-trending Ramapo and Reservoir fault zones were initially established during the earliest phase of the Grenville orogeny as ductile reverse faults. In the later phase, both zones were reestablished as ductile strike-slip faults. The shear sense is unequivocally dextral, evidenced by the multiple kinematic indicators such as S-C fabrics, rotated porphyroclasts, and asymmetric boudins. Evidence is also present for multiple subsequent reactivations, including later ductile and brittle fabrics.

Late in the Grenville cycle, a ~35 km wide zone of anastomosing near vertical mylonite zones overprinted early shallowly dipping foliations. Locally, shear zones in the western Hudson Highlands became dilational and extensive alteration and vein mineralization occurred. The veins formed in dilational right step-over jogs during the late stages of movement in northeast trending dextral shear zones. Locally buffered fluids controlled mineralization, resulting in calc-silicate, ferromagnesian, and quartz-sulfide assemblages. This process produced three zones: 1) a 'bleached' zone of altered wall rock adjacent to the vein, 2) an outer 'layered' zone in the vein, of ferromagnesian-rich bands, and 3) a core of massive magnetite ore and secondary minerals.

## INTRODUCTION

The Reading Prong is a Grenville basement massif that forms part of the spine of the Appalachians, connecting the Blue Ridge and Green Mountain provinces, in Pennsylvania, New Jersey, New York, and into Connecticut (Fig. 1). It is composed of Grenville aged crystalline rocks that have largely been metamorphosed to granulite facies (see Drake, 1984). The Reading Prong is bounded to the west by deformed Paleozoic sedimentary rocks of the Valley and Ridge Province and to the east by the Piedmont Province. Known as the New Jersey Highlands and the Hudson Highlands in New York, it boasts a complex deformational history of multiple reactivations. The rocks of the highlands are interpreted to have formed in an island arc or magmatic arc as volcanics, volcaniclatics, and sedimentary rocks.

The details of the Grenvillian orogeny in the Appalachians are commonly difficult to decipher because of complex structural relations, lack of exposure, and pervasive granulite facies metamorphism, as well as extensive structural and metamorphic overprinting during the Paleozoic and Mesozoic locally (Ratcliffe, 1972; Bartholomew and Lewis, 1988; Krol *et al.*, 1992; Krol and Zeitler, 1994; Gates *et al.*, 2006). Gates (1995; 1998) and Gates and Costa (1998) proposed a major late Grenvillian dextral strike-slip event in the Reading Prong. This shearing was constrained to discrete faults, such as the Ramapo and Reservoir faults (Gates *et al.*, 2004), which were active well after peak Grenville tectonism and to lower temperatures (Gates *et al.*, 2006)(Fig. 2). Fundamental zones of crustal weakness that were established were reactivated multiple times during subsequent tectonic events. The rocks in these fault zones contain complexly overprinted mylonites, cataclasites, and breccias with distinct kinematics and mineralizations (Gates and Costa, 1998). Bimodal (diorite and granite) plutons intruded the area prior to the onset of a steeply southeast-dipping ~35 km wide dextral shear system that resulted from tectonic escape (Gates *et al.*, 2006).

The second event produced discrete zones of ductile deformation with a consistent dextral strike-slip shear sense and crenulation cleavage (Gates, 1998). Steeply southeast- to northwest-dipping 1 to 3 km wide zones of mylonite display extensive shallow northeast trending lineations, S-C fabrics, asymmetric boudins, asymmetric intrafolial folding, and rotated porphyroclasts locally (Gates, 1998). Late in their history, the shear zones crossed the brittle ductile transition and became dilational where extensive iron mineralization locally accompanied the shearing. Iron mineralized as magnetite veins in several shear zones exposed in the western Hudson Highlands following extensive fluid alteration of country rock and gauge mineral mineralization late in the Grenville orogenic cycle (Kalczynski and Gates, 2014). The veins are exposed at several abandoned magnetite mines within Harriman State Park. New modeling for the mode of formation of these magnetite deposits is discussed as well as reactivation history of the Ramapo and Reservoir fault zones.

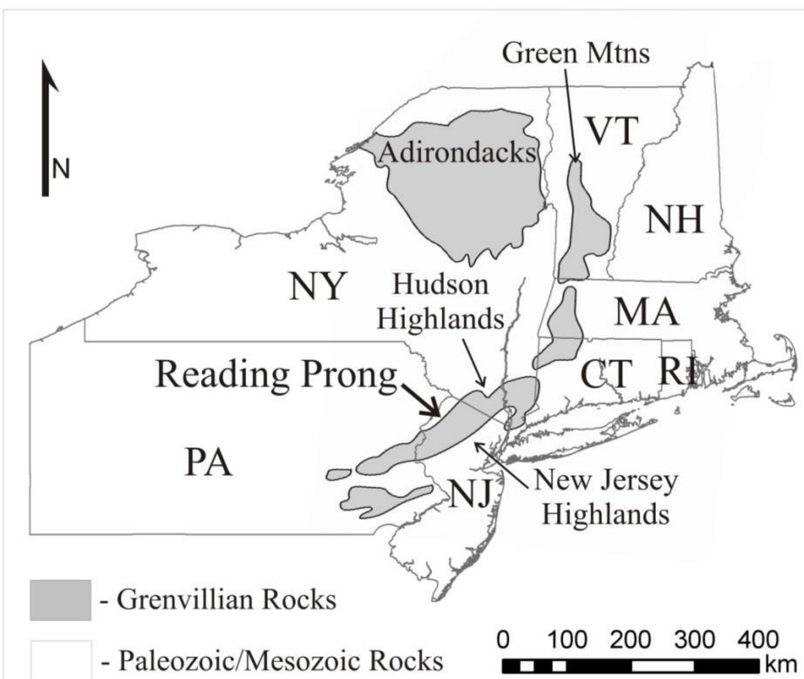


Figure 1. Map of the Northeastern United States showing distribution of Appalachian/Grenville rocks, the Reading Prong, and the Hudson and New Jersey Highlands.

# GEOLOGY OF THE NEW JERSEY AND HUDSON HIGHLANDS

Several models currently exist for the formation of the crystalline bedrock of the Hudson Highlands. Recent geochemical investigations found that some of the rocks are of plutonic origin (Gundersen, 2004; Volkert and Drake, 1999; Volkert, 2001; Gates *et al.*, 2006), but based upon major element geochemistry, some of the layered gneisses have been interpreted to be volcanic (Helenek, 1971; Drake, 1984; Puffer and Gorring, 2005; Gates *et al.*, 2006). Gundersen (2004) and Volkert *et al.* (2010) proposed that many of these gneisses formed in an extensional backarc marginal basin, with a bimodal, volcanic origin whereas Gates *et al.* (2006) proposed formation of a volcanic pile with a volcaniclastic apron in an island arc or marine magmatic arc setting.

According to Gates *et al.* (2006), a volcanic pile initiated in an arc setting around 1.29 to 1.25 Ga (Volkert *et al.*, 2010), and is characterized by layered intermediate and mafic rocks, associated plutons, and volcaniclastic sediments. Continental collision of the arc with another continent (likely Amazonia) occurred during the building of the Rodinian supercontinent, ~1,050 to 1,020 Ma (Gates *et al.*, 2006). This sequence underwent granulite facies metamorphism, between 1,045 to 1,024 Ma associated with the Ottawan phase of the Grenville orogeny (Volkert *et al.*, 2010). Locally, anatexis produced migmatites, granite sheets, and the early pegmatites (Gates *et al.*, 2006). Subsequent diorite intrusions occurred around 1,008 Ma either the result of delamination at the end stages of the collision event, or the early dilational stages of a second tectonic event (Gates *et al.*, 2006). This second event is characterized by dextral strike-slip movement during a period of rapid uplift and unroofing at approximately 1,008 to 924 Ma (Gates and Krol, 1998). A ~35 km wide zone of anastomosing near vertical mylonite zones overprinted early shallowly dipping foliations. Total dextral offset was on the order of several hundred kilometers (Gates *et al.*, 2006).

Previous geologic mapping in this region sub divided gneisses based upon the individual varietal ferromagnesian minerals (Dodd, 1965; Dallmeyer, 1974). Considering that 80% of these rocks are quartzofeldspathic gneisses (Gates *et al.*, 2006), this paper follows the system proposed by Gundersen (1986), and adapted by Gates *et al.* (2006). Units are grouped into lithofacies based on various rock types, to define quartzofeldspathic, interpreted metasedimentary (calc-silicate, metapelite, and metapsammite), and metavolcanic (plagioclase-amphibole-pyroxene) assemblages.

## Metavolcanic Gneiss

The metavolcanic unit consists of strongly banded sequences of inter-layered mafic and intermediate gneisses, with interpreted volcanic protoliths (Gates *et al.*, 2006). Compositional banding ranges in thickness from 5 cm to 5 m with varying quantities of each rock type. Mafic assemblages are composed primarily of medium to coarse grained amphibole, plagioclase, clinopyroxene and orthopyroxene, with minor sulfides and magnetite locally. Intermediate bands are primarily medium to coarse grained plagioclase and quartz, with minor amounts of amphibole, biotite, clinopyroxene and orthopyroxene. This unit also contains localized interlayers of interpreted metasediments such as, quartzite, marble, and calc-silicate gneiss, as well as migmatites. The contacts with the quartzofeldspathic unit are interstratal gradational.

## Quartzofeldspathic Gneiss

The quartzofeldspathic gneiss ranges from massive to layered quartz-plagioclase gneiss to quartz-K-feldspar-plagioclase gneiss with lesser amounts of clinopyroxene, orthopyroxene, amphibole, and/or biotite. Minor amounts of magnetite and garnet also occur locally. Compositional layering is defined by the proportions and species of ferromagnesian minerals. At the contact with the metavolcanic unit, it is also locally interlayered with quartzite and amphibole-pyroxene gneiss. Gradational contacts with the metavolcanic lithofacies, composition and mineralogy, and internal compositional layering suggest that this unit represents a volcaniclastic sequence (Gates *et al.*, 2006). Zircons analyzed from the quartzofeldspathic unit yield ages between 1,160 – 1,220 Ma for the zoned cores and between 1,000 - 1,080 Ma for the clear rims (Gates *et al.*, 2006).

## Metasedimentary Gneiss

Throughout the western Hudson Highlands there are belts of rock considered to have sedimentary protoliths including metapelite, metapsammite, and calc-silicate gneisses interlayered with quartzite and marble. Belts of rock contain varying amounts of these lithologies interlayered at the scale of meters to hundreds of meters (Gates *et al.*, 2006). The calc-silicate gneiss is quartzofeldspathic containing diopside, K-feldspar, fluorapatite, titanite, scapolite, and amphibole. Tens of centimeters to meter-scale quartzite layers and discontinuous layers of diopside marble also occur in this unit. The metapelite consists of interlayered biotite-garnet gneiss with medium to coarse quartz, plagioclase, K-feldspar, and cordierite and sillimanite locally (Gates *et al.*, 2006). Zircons analyzed from the metasedimentary units yielded ages between 1,100 – 2,800 Ma for the zoned detrital cores and between 1,000 – 1,030 Ma for the distinct metamorphic rims (Gates *et al.*, 2006).

## Diorite

Coarse to very-coarse grained black and white diorite dikes and bodies containing plagioclase, orthopyroxene, clinopyroxene, interstitial amphibole, and minor biotite, occur throughout the field area. Hornblende rims clinopyroxene which armors orthopyroxene, however orthopyroxene does not occur within sheared diorite. The diorite also grades to pyroxene-poor, anorthositic compositions locally (Gates *et al.*, 2003). Multiple small bodies of diorite are concentrated in certain areas, possibly indicating larger bodies at depth (Gates *et al.*, 2006).

Textures vary from coarse granoblastic to foliated and mylonitic with type II S-C fabrics (Lister and Snoke, 1984), exhibiting dextral shear sense (Fig. 2). Locally, the diorite contains xenoliths of gneiss, showing ductile contacts which are partially melted, forming a rind of coarse pegmatite granite. Granite also fills fractures in the diorite that opened after crystallization, but while the granite was still liquid (Gates *et al.*, 2006). Subhedral zircons with minimal to no zoning yielded a cluster of ages averaging 1,008 +/- 4 Ma (Gates *et al.*, 2006).

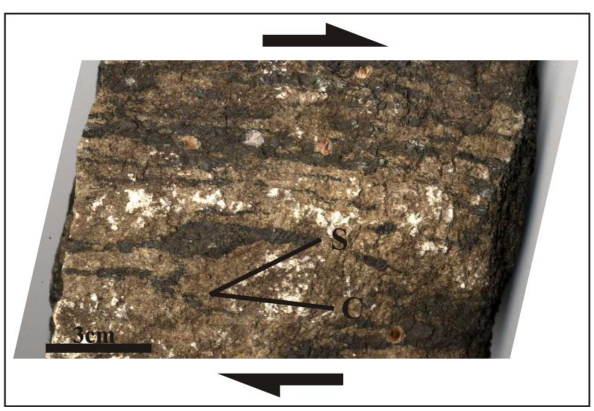


Figure 2. Lake Tiorati Diorite, with type II S-C fabrics and σ porphyroclasts indicating dextral shear sense.

### Pegmatites

Two generations of pegmatites occur throughout the field area. The earliest dikes are white and contain K-feldspar, quartz, muscovite and minor garnet locally. They are concordant to semi-concordant to the gneissic foliation, commonly boudinaged and contain internal fabrics and deformed grains. Thickness of these dikes ranges from 1 cm to 1 m. The later pegmatitic dikes are pink and very coarse grained, containing K-feldspar and quartz with muscovite, amphibole, magnetite, pyroxene, titanite, and/or garnet locally, depending on the rock intruded. They are highly discordant, commonly within brittle faults and contain xenoliths of gneiss, mylonites, and mineralized rock. They show minor to no deformational fabrics, and thickness ranges from 1 to 10 m. They are also associated with small granite bodies (Gates *et al.*, 2006). Ar/Ar thermochronology of hornblende from the later pegmatite yielded an age of 923 +/- 2.8 Ma, and an age of 794 +/- 3.0 Ma from biotite samples (Gates *et al.*, 2006).

## REACTIVATED ZONES OF THE NEW JERSEY HIGHLANDS

### Ramapo Fault

The Ramapo fault zone is the boundary between the eastern and central highlands (Fig. 3). The northeast-trending Ramapo fault system in northern New Jersey and southeastern New York juxtaposes Middle Proterozoic crystalline rocks of the Reading Prong with Triassic and Jurassic sedimentary and igneous rocks of the Newark Basin along most of its length. The Ramapo fault system varies in thickness from approximately 5 km to 10 km along strike (Ratcliffe, 1980). It consists of many parallel to subparallel zones of well foliated to poorly to moderately lineated type II S-C mylonite (Lister and Snoke, 1984) and ultramylonite in Grenville gneisses (Fig. 4)(Gates and Costa, 1998). Primary kinematic indicators from the mylonite along the Ramapo fault system in northern New Jersey consistently exhibit reverse shearing sense, indicated by both σ-type and δ-type quartz porphyroclasts (Fig. 4B)(Passchier and Simpson, 1986).

Cores of the porphyroclasts define the southeast-dipping S plane and have tails of dynamically recrystallized quartz. Type B2a and type B2b quartz ribbons (Boullier and Bouchez, 1978) and dynamically recrystallized tails on porphyroclasts (Passchier and Simpson, 1986) define the C plane (Gates and Costa, 1998). The C' Plane, where present, is defined by asymmetric boudinage of quartz ribbons (Gates and Costa, 1998). Potassium feldspar and plagioclase also form σ-type and δ-type porphyroclasts (Fig. 4A)(Passchier and Simpson, 1986) with tails of recrystallized feldspar, quartz, muscovite and chlorite (Costa and Gates, 1998). Cores of these porphyroclasts also define the southeast-dipping S plane. The C plane is defined by porphyroclast tails. Edges of the feldspar porphyroclasts are commonly dynamically recrystallized (Gates and Costa, 1998). Plagioclase porphyroclasts have deformed twin lamellae. Feldspar porphyroclasts, less commonly, show pull-apart textures (Stauffer, 1970) that show antithetic shearing along cleavage planes (Gates and Costa, 1998). The ductile behavior exhibited by the feldspar porphyroclasts, indicates that the temperatures of this phase of deformation were in excess of 450 ± 50°C (Sibson, 1977; 1983; Tullis and Yund, 1977). This mineral response is consistent with deformation at middle to upper greenschist facies conditions (Simpson, 1985) (Gates and Costa, 1998).

C planes typically dip 40 to 50° towards the southeast. The average angle between S and C planes is 20°, but varies from 6 to 40°. C' planes where present, are spaced from 1.0 mm to 1.0 cm and oriented approximately 20 - 30° shallower than the C plane. Lineations of quartz, amphibole, and chlorite are consistently down dip (Gates and Costa, 1998). Chlorite and muscovite "fish" (Eisbacher, 1970; Lister and Snoke, 1984) and aligned muscovite; tremolite and biotite define the southeast-dipping S-C fabric as well. Biotite commonly underwent reaction enhanced ductility (White *et al.*, 1980). C’ planes commonly developed within the chlorite-rich zones (Gates and Costa, 1998).

Hornblende commonly underwent a brittle response. Pull-apart (Stauffer, 1970) hornblende porphyroclasts underwent reaction-enhanced ductility (White *et al.*, 1980) in which crude σ-type porphyroclasts evolved from antithetically sheared fragments. In these retrograded grains, metamorphic reactions generated chlorite, tremolite-actinolite, biotite, and muscovite as fillings within conjugate shear planes and as tails on porphyroclasts (Gates and Costa, 1998). The tails on some of the quartz porphyroclasts are pulled under or over the grain in a direction opposite to that indicated by the porphyroclasts. Some of the brittle hornblende grains show pull-apart textures with a shear sense opposite to that of the mylonitic matrix. Within some of the hornblende grains, the fractures formed during extension and fragmentation of the grain are V-shaped and are syntaxially filled first by amphibole and then by a chlorite-muscovite-quartz intergrowth. The amphibole is parallel to the fracture walls and indicates no rotation whereas the second growth indicates substantial rotation. V-textures could be used as kinematic indicators in single deformations (Hippert, 1993), but the textures described here are clearly composite and indicate a complex history (Gates and Costa, 1998).

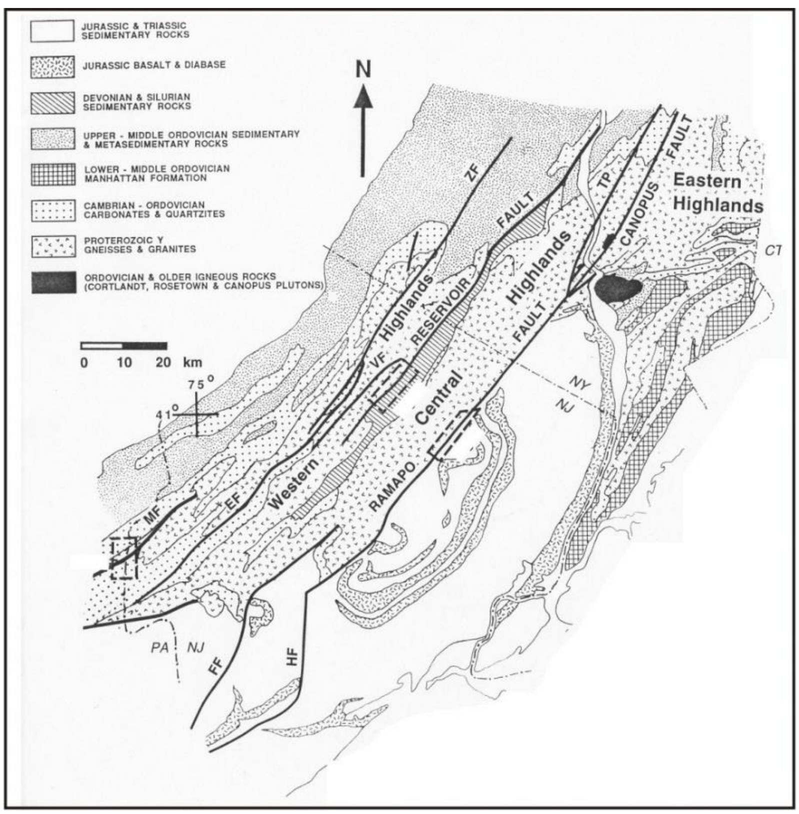

Figure 3. Geologic map of the northern Reading Prong, NY, NJ, and Pa, showing locations of the Ramapo and Reservoir faults (from Gates and Costa, 1998).

Within these mylonite zones of reverse movement, there is evidence for an earlier phase of normal movement at approximately the same metamorphic grade. Features such as intrafolial rootless isoclines and relict foliations, composite porphyroclasts, and V-shaped fractures with two syntaxial overgrowths (Fig. 4C) support this interpretation (Gates and Costa, 1998). The intrafolial folds and relict foliations occur primarily within quartz ribbons but also in within the fine-grained mylonitic matrix. Some porphyroclasts and brittle pull apart grains exhibit evidence for two periods and directions of movement (Gates and Costa, 1998).

In addition to its development as a Grenville reverse fault (Ratcliffe, 1980), the Ramapo fault system has a long and complex reactivation history which includes up to five periods of fault movement. The dominate reverse ductile deformation which resulted in the development of the southeast dipping type II S-C mylonite (Fig. 4D) (Lister and Snoke, 1984) and ultramylonite zones is post-Grenville in age. The mineralogy and texture which are present are indicative of a lower grade deformation than those reached during the Grenville orogeny. Based on the deformation features and metamorphic grade of deformation (Simpson, 1985), the reverse mylonites and ultramylonites within the study area formed at mid- to upper greenschist metamorphic facies (Gates and Costa, 1998).

Cataclastic textures (Sibson, 1977) that overprint the early ductile and brittle-ductile fabrics indicate brittle strike-slip and normal reactivation of the southeast-dipping faults. Cataclastic seams (0.5 mm to 1.5 cm thick) offset grains and early fabrics are themselves offset by later faults (Gates and Costa, 1998). Southeast-dipping foliated greenish-gray to black gouge zones approximately 4.0 to 5.0 cm thick are commonly enriched in calcite and sheared antithetically (Gates and Costa, 1998). In addition, there are two generations of type I (Beach, 1975) quartz, calcite, and chlorite filled tension gashes and two generations of primary and secondary (Harding, 1974) planar, curvi-planar and listric brittle fault arrays with slickenlines (Gates and Costa, 1998).

Slickenside coated fault surfaces most commonly contain fibrous or stepped slickenlines of fine grained chlorite, tremolite-actinolite, limonite and calcite with lesser amounts of quartz and epidote. Two generations are evident by overprinting relations on single fault surfaces (Gates and Costa, 1998). Each generation of brittle faults includes four sets of moderate to steeply dipping faults. The early generation of steeply-dipping brittle faults includes east-southeast and west-northwest-dipping reverse faults; northeast and southwest-dipping normal faults and a conjugate set of north-northwest and south-southeast-dipping right-lateral strike-slip and east and west-dipping left lateral strike-slip faults. The later set of brittle faults includes south-southwest and north-northwest-dipping reverse faults, southeast and northwest-dipping normal faults and a conjugate pair of northeast and southwest-dipping right-lateral strike-slip and southeast-dipping left-lateral strike slip faults. An additional set of northwest and southeast-dipping right lateral strike-slip faults is present. Fault planes also developed P and T criteria kinematic indicators (Petit, 1987) and tension gashes filled with calcite, tremolite-actinolite, chlorite, and quartz (Gates and Costa, 1998).

The dominant ductile reverse mylonite fabric overprints a previously developed normal mylonitic fabric interpreted to be the result of Iapetan rifting as it predates Taconian deformation and postdates Grenville deformation (Gates and Costa, 1998). A Taconian age (450 – 460 Ma) has been assigned to reverse ductile movement on the Ramapo fault zone of southeastern New York based radiometric dates of plutonic and dike rocks of the Rosetown pluton and Cortlandt Complex (Ratcliffe, 1980; 1981; Ratcliffe *et al.*, 1982). During post-Ordovician and pre-Mesozoic activity mesoscopic synchronous primary and secondary brittle faults (Harding, 1974) and associated tension gashes (Costa, 1991) developed within the Ramapo fault system showing both reverse and strike-slip motion (Costa and Gates, 1998). Costa and Gates (1993) interpreted the strike-slip and reverse motion to be of the same generation and Alleghanian in age based on regional relations.

Overprinting slickenlines on a single fault plane allow the determination of a younger generation of brittle faults superimposed over the interpreted Alleghanian generation. This brittle phase of deformation corresponds with the southeast dipping normal faults which created the Newark basin (Gates and Costa, 1998). The Mesozoic sediments (Olsen, 1980) within the basin constrain the time of faulting. During Mesozoic rifting primary and secondary brittle faults (Harding, 1974) and associated tension gashes also developed (Gates and Costa, 1998). The generation of overprinting cataclastic textures and fault gouge (Sibson, 1977) indicate faulting was under low temperature (<250°C) and shallow conditions (<10 km). An approximate north-northeast-trending maximum compressive direction is indicated by the complex fault array and tension gashes, requiring that the formation of the Newark basin had a transtensional component (Gates and Costa, 1998).

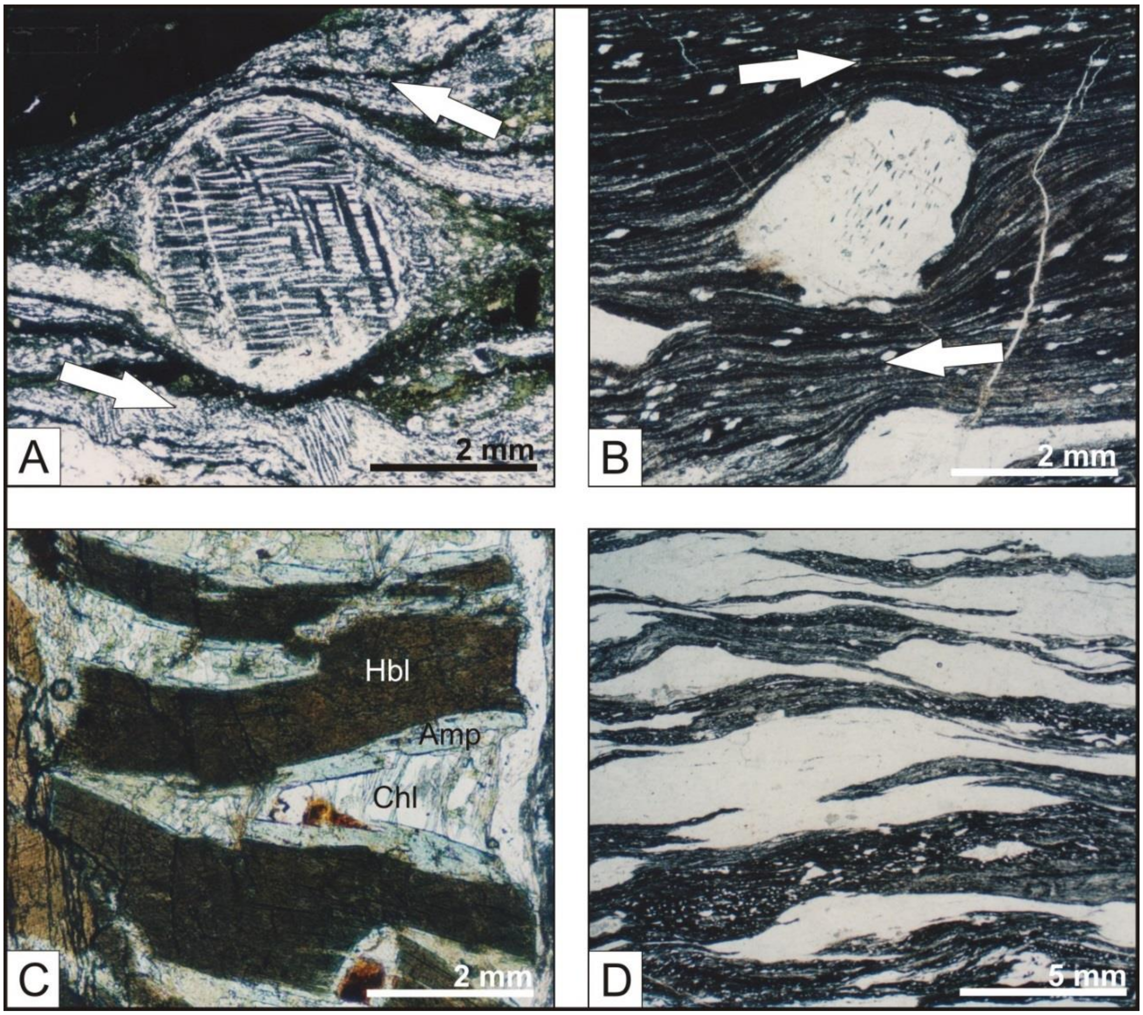


Figure 4. Photomicrographs of rocks from the Ramapo fault zone. Arrows show shear sense. A) Rotated porphyroclast of microcline. B) Rotated quartz porphyroclast. C) V-shaped fracture in a pull-apart hornblende porphyroclast. Composite filling of early amphibole and late chlorite-sericite-quartz intergrowth. D) S-C mylonite showing mylonitic fabric, quartz ribbons, and rotated quartz porphyroclasts.

## Reservoir Fault

The Reservoir fault marks the boundary between the central and western Highlands. The shear zone is best developed in the Grenville gneisses of the Losee metamorphic suite (Lewis and Kummel, 1912; Hague *et al.*, 1956; Drake, 1984; Gates, 1993). The Reservoir fault is a multiply activated zone of weakness that forms the western boundary of the Silurian-Devonian Green Pond outlier. The vertical to steeply northwest- and southeast-dipping shear zone extends from the Hudson Highlands, New York into the central New Jersey Highlands. Cataclastites and mylonites are best developed around Newfoundland, New Jersey within Grenville paragneisses that have been interpreted as being of metasedimentary origin (Lewis and Kummel, 1912; Hague *et al.*, 1956; Drake, 1984; Volkert, 1993). These rocks are dominantly layered amphibole, biotite, and pyroxene quartzofeldspathic gneisses and minor amphibolite gneiss (Gates and Costa, 1998). The quartzofeldspathic gneiss is interpreted as being derived from layered volcaniclastic and calcsilicate rocks (Drake, 1984; Gundersen, 1986) and contains scapolite, pyroxene, and garnet assemblages or plagioclase-pyroxene-amphibole-garnet assemblages (Malizzi and Gates, 1989). The gneisses were intruded by uraniferous pegmatite dikes along the Reservoir fault subsequent to or during granulite facies metamorphism (Malizzi and Gates, 1989).

Protoliths of the Reservoir fault rocks are preserved along the western margin of the fault and as xenoclasts and xenocrysts within the fault zone. The protolith is primarily a granitic to tonalitic paragneiss with antiperthite, varietal edenite to hornblende, and/or diopside and minor ilmenite, and apatite with a granoblastic to gneissic texture (Gates and Costa, 1998). Locally these rocks preserve early mylonitic textures. The amphibole in this rock is F-rich (1.5-2.0 wt.%) and Cl-bearing (up to 0.5 wt.%) (Gates and Costa, 1998). Feldspar is albite with exsolution lamellae of K-spar. There are also minor amounts of pyroxene-bearing amphibolite. In the fractured gneisses adjacent to the main fault zone, plagioclase, edenite-hornblende and locally, diopside are replaced by F-magnesiohastingsite along fractures and cleavage plains (Gates and Costa, 1998). Typically, the most complete replacement occurs closest to the fracture but, in many cases, the new mineral permeates the entire grain. Illmenite has overgrowths of titanite (Gates and Costa, 1998).

Brittle deformation of the granitic-tonalitic gneiss ranges from veining and fracturing in rocks adjacent to the fault to extensive fault breccia and cataclasite within the fault zone. Feldspar are fractured or granulated and commonly offset along microfaults that exploit mineral cleavage plains (Gates and Costa, 1998). The fractures are filled with amphibole, epidote, calcite, chlorite, and hematite. Quartz shows extreme lattice misorientation, much of which likely reflects submicroscopic cataclasis (Tullis and Yund, 1987) with minimal plastic deformation (Gates and Costa, 1998). Quartz also exhibits extensive fractures that are filled with essentially the same minerals as feldspar. Other minerals are offset along fractures and show extensive reaction textures (Gates and Costa, 1998).

In the mylonitic part of the shear zone, xenoclasts, xenocrysts, and coarse-grained neomineralized amphibole cores exhibit brittle deformation whereas fine-grained amphibole and chlorite display marginal plastic deformation (Gates and Costa, 1998). A well-developed S-C mylonitic fabric is formed in the amphibole-rich matrix including late C' planes (Simpson and Schmid, 1983). S planes are composed exclusively of fine-grained magnesiohstingsite and the cores of magnesiohstingsite porphyroclasts whereas C and C' planes are fine-grained ferro-actinolite and actinolite with variable amounts of chlorite (Gates and Costa, 1998).

Larger grains of F-magnesiohastingsite including porphyroclasts cores commonly exhibit varying amounts of brittle fracturing primarily as microfaulting along cleavage planes and subsequent bending of the microfault blocks with Cl-magnesiohstingsite and chlorite filling the fractures. These large grains also commonly exhibit mantles and asymmetric tails of fine-grained and aligned Cl-magnesiohstingsite, ferro-actinolite and actinolite and form rotated σ-type (Gates and Costa, 1998). According to Gates and Costa (1998), seemingly solid cores of F-magnesiohastingsite porphyroclasts show that most of the rims and even inner cores, in some cases, are granulated and overgrown by epitaxial Cl-magnesiohastingsite with 1.0 to as much as 2.4 wt.% Cl but with little to no F. The outer edge of the porphyroclast in turn is rimmed by ferro-actinolite and actinolite. The S-C fabric, rotated porphyroclasts, and offset brittle grains including pull-aparts consistently show a dextral transcurrent sense of shear (Gates and Costa, 1998).

Overgrowths and fracture fillings on Cl-magnesiohastingsite are optically continuous ferro-actinolite and actinolite and subsequently actinolite + chlorite. Unlike the magnesiohastingsite, the ferro-actinolite is more commonly intergrown with other minerals (Gates and Costa, 1998). Assemblages include fine-grained epidote, albite, titanite, apatite, pyrite, and locally muscovite and biotite but they are still dominated by amphibole. These minerals occur in shear bands and in veins that parallel foliation. Biotite also shows a transition from F-rich to Cl-rich compositions within ferro-actinolite and actinolite bearing assemblages (Gates and Costa, 1998).

Small pockets within the fault zone contain extensive breccia and cataclasite that lack foliation. The matrix of these rocks is primarily actinolite. In the well-developed cataclasite parts of the shear zone, rounded xenoclasts of both protolith and cataclastic fault rock range up to 0.5 m but most relict components are 0.5 to 1.0 mm xenocrysts of quartz and feldspar. The xenoclasts and xenocrysts float in a matrix of randomly oriented 0.1 to 0.5 mm actinolite with minor chlorite, biotite, albite, apatite, epidote and rare pyrite (Gates and Costa, 1998).

The retrograde metamorphism that accompanied shearing is reflected in mineralogical changes. The observed protolith assemblages in granitic-tonalitic gneiss are: diopside + low Ca feldspar (antiperthite) + quartz + ilmenite, or edenite-hornblende + low Ca feldspar (antiperthite) + ilmenite ± scapolite ± garnet (Gates and Costa, 1998). These assemblages were produced during peak granulite facies metamorphism. The first retrograde assemblage is magnesiohastingsite which is locally potassian and consistently a flouro-amphibole + titanite ± albite ± pyrite (Gates and Costa, 1998). Amphibole makes up about 90 to 95% of this assemblage. The early magnesiohastingsite is F-rich but subsequent magnesiohastingsite became progressively more Cl-rich. Amphibole analyses with equal parts of F and Cl (~1%) are common (Gates and Costa, 1998). The latest magnesiohastingsite observed is Cl-rich and contains no F. These data indicate that metamorphic fluids underwent a transition from F-rich to Cl-rich compositions that was synchronous with movement on the Reservoir fault (Gates and Costa, 1998). Ferro-actinolite-rich assemblages succeeded the magnesiohastingsite assemblages and include albite, epidote, titanite, apatite, biotite, and chlorite. The final retrograde amphibole is actinolite and it is virtually always associated with chlorite in varying proportions (Gates and Costa, 1998). Other common associations include epidote, apatite, albite, titanite, and biotite. These later assemblages are most common in cataclasites with random grain orientations (Gates and Costa, 1998).

The Reservoir fault zone has a history of multiple periods of activity. Previous workers have suggested that it underwent Alleghanian movement (Hull *et al.*, 1986; Mitchell and Forsythe, 1988), and that it is still active, producing regular low magnitude earthquakes (Ratcliffe, 1980). It has been proposed to have had Mesozoic (Lewis and Kummel, 1912), Acadian (Finks, 1990), Taconian (Ratcliffe, 1980), and some form of Precambrian movement (Hull *et al.*, 1986), but these phases of motion are not as easily documented (Gates and Costa, 1998).

Based on overprinting relations, the mechanical response of the minerals and the chlorite-bearing assemblages of the fault rocks, shearing postdated peak granulite facies metamorphism associated with the Grenville orogenesis (Gates and Costa, 1998). Because quartz appears to straddle the brittle-ductile transition, the temperature of deformation of this strike-slip event appears to have been approximately 300 ± 50°C (Tullis and Yund, 1977) or less, which is consistent with the chlorite + actinolite + albite assemblages (Gates and Costa, 1998). On the other hand, the presence of F-rich fluids and halogen-rich fluids in general indicates that it is related to Proterozoic metamorphism (Gates and Costa, 1998). The edenite and hornblende in the protolith Reservoir fault rocks have similar F contents to the F-magnesiohastingsite within the fault rocks. Such high F contents and halogen content in general are common in amphiboles and biotite within rocks that underwent Grenville metamorphism in the Reading Prong (Gundersen, pers. comm., 1994). Such concentrations of halogen-rich amphibole within fault zones or otherwise do not occur within the Paleozoic sedimentary rocks of the Green Pond outlier (Gates and Costa, 1998). Other occurrences of amphibole mineralization within the New Jersey Highlands are also restricted to late fault zones within crystalline rocks (Kalczynski and Gates, 2014), though Paleozoic sedimentary rocks are common in the area. Based on occurrence and composition, the movement accompanying amphibole mineralization on the Reservoir fault is late Middle to Late Proterozoic in age (Gates and Costa, 1998).

Because movement sense is unequivocally dextral, it is likely late Middle Proterozoic (Gates and Costa, 1998). Costa and Gates (1993) have identified normal movement on the nearby and parallel Ramapo fault. They propose that this movement is Late Proterozoic to earliest Cambrian and related to the opening of the Iapetus. These results are consistent with the interpretation of Iapetan rift deposits of Drake (1984) in the western Reading Prong. Based on orientation, inferred orientation of the maximum compression direction, and regional relations, the dextral strike-slip faulting on the Reservoir fault is more consistent with the earlier movement on the Ramapo fault (Ratcliffe *et al.*, 1972) than Iapetan rifting although oblique extension cannot be ruled out (Gates and Costa, 1998).

The timing of the multiple movement periods on the Reservoir Fault is poorly constrained by both geochronology and the stratigraphy of the area (Gates and Costa, 1998). Clearly the dominate deformation in the Green Pond outlier is Late Paleozoic Alleghanian and compressional in nature (Hull *et al.*, 1986; Mitchell and Forsythe, 1988; Herman and Mitchell, 1991) and the Reservoir fault was certainly active during this event (Gates and Costa, 1998). Malizzi and Gates (1989) proposed that this movement may have been dextral transpressional rather than simply compressional. Hull *et al.* (1986) and Malizzi and Gates (1989) speculated on Grenvillian movement on the fault, possibly recorded by gneissic foliation and aligned uraniferous pegmatites. The Reservoir fault was active several times during the Paleozoic and Mesozoic (Gates and Costa, 1998). Ratcliffe (1980), Mitchell and Forsythe (1988) and Malizzi and Gates (1989) documented two post-deformational phases of movement, one of which preserved the Green Pond outlier through west-side-up movement. Lewis and Kummel (1912) and Ratcliffe (1980) considered the entire Green Pond outlier to be preserved in a Mesozoic graben, the Reservoir fault having had normal movement. Finks (1990) proposed that the thick, high energy Devonian sedimentary rocks were deposited in a restricted dextral transtensional pull-apart basin, accounting for its separation from the Catskill depocenter to the west (Gates and Costa, 1998). Ratcliffe (1980) proposed Taconian movement on the zone as well as neotectonism, marked by the low intensity of earthquakes

## MINERALIZED ZONES OF THE HUDSON HIGHLANDS

Within the western Hudson Highlands, half-kilometer wide shear zones, formed within the ~35 km-wide anastomosing dextral strike-slip shear system (Gates *et al.*, 2004), and contain concordant to slightly discordant mineralized ore veins (Fig. 5). The northeast trending zones are defined by steeply dipping foliations, penetrative mineral lineations, and type II S-C mylonites with dextral kinematic indicators (Fig. 2). The vein-wall rock contact is generally sharp and semi-concordant to the mylonitic foliation, but slightly discordant and uneven locally.

The veins and their contacts are characterized by three distinct zones sub-parallel to the wall rock boundary (Fig. 6). The unaltered wall rock, grades into a 1 to 2 cm thick ‘bleached zone’ that is lighter in color and marked by the alteration of the original wall rock minerals. The bleached zone is in contact with the mineralized vein. The bleached zone is not uniformly distributed throughout the deposits, and in some areas the mineralized vein is in direct contact with wall rock.

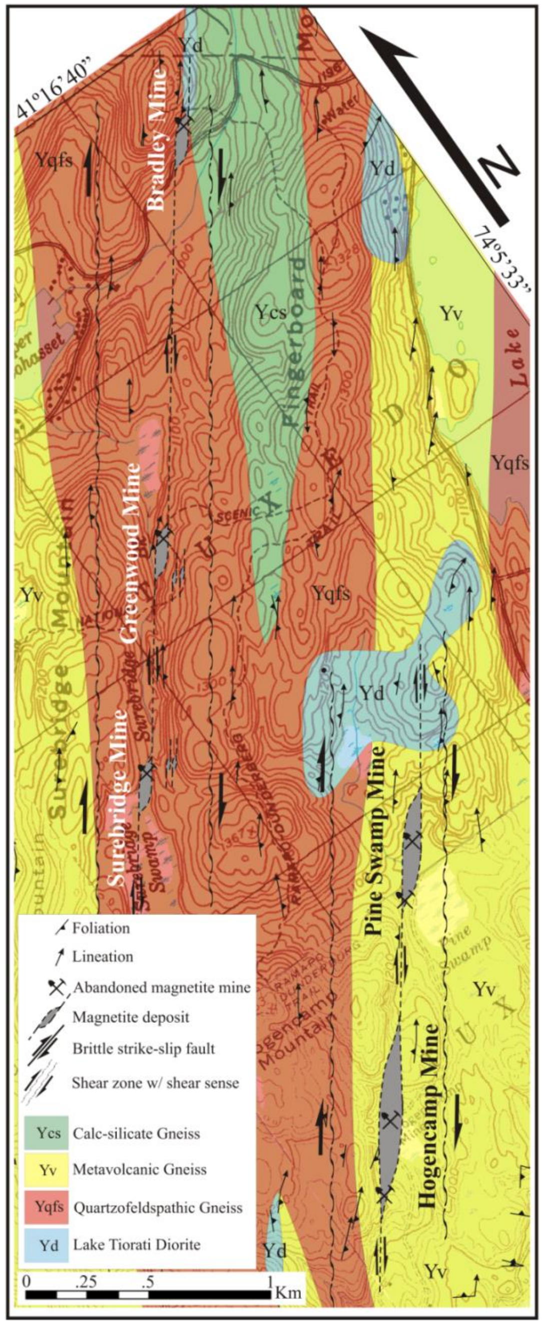


Figure 5. Geologic map of the Hudson Highlands study area, located within Harriman State Park, NY.

The mineralized vein is characterized by two distinct zones, a layered sequence adjacent to the wall rock and a core of primarily very coarse, massive minerals (>2 cm). The layered sequence is characterized by distinct, dark colored bands of fine to medium grained, pyroxene, amphibole, and/or biotite-rich assemblages, which range in thickness from 2 to 10 cm and have gradational to sharp contacts. The cores of the veins are characterized by medium to very coarse, magnetite ore, randomly oriented amphibole and pyroxene gangue minerals, and late stage interstitial cementing minerals (Fig. 7). Thickness of the vein ranges from 2 to 15 m and length is ~10 m to 1 km. The thickness of the ore zone ranges from 1 to 10 m and length is ~100 to 500 m. The narrow zones that connect the magnetite deposits are typically composed of randomly oriented to aligned pyroxenes and amphiboles with minor magnetite, biotite, and/or quartz. The zones are commonly intruded by late pegmatite dikes that contain the mineralized rock as xenoliths.

Bleached zone mineral assemblages, vein material, and late-stage cementing minerals vary by location within the mineralized zones. In areas of calcium-rich country rocks, clinopyroxene/calcite rich mineral assemblages dominate the bleached zone and the vein assemblages. In areas of quartzofeldspathic country rock, amphibole/quartz assemblages dominate the layered and massive vein material, whereas areas with iron and sulfide-rich country rocks (metavolcanics), contain orthopyroxene/sulfide-rich vein assemblages. Pyroxenes vary by location between diopside, and iron-rich orthopyroxenes, whereas amphiboles are mainly chlorine- and fluorine-rich magnesiohastingsite (Gates, 1995) and potassichastingsite (Lupulescu *et al.*, 2009).

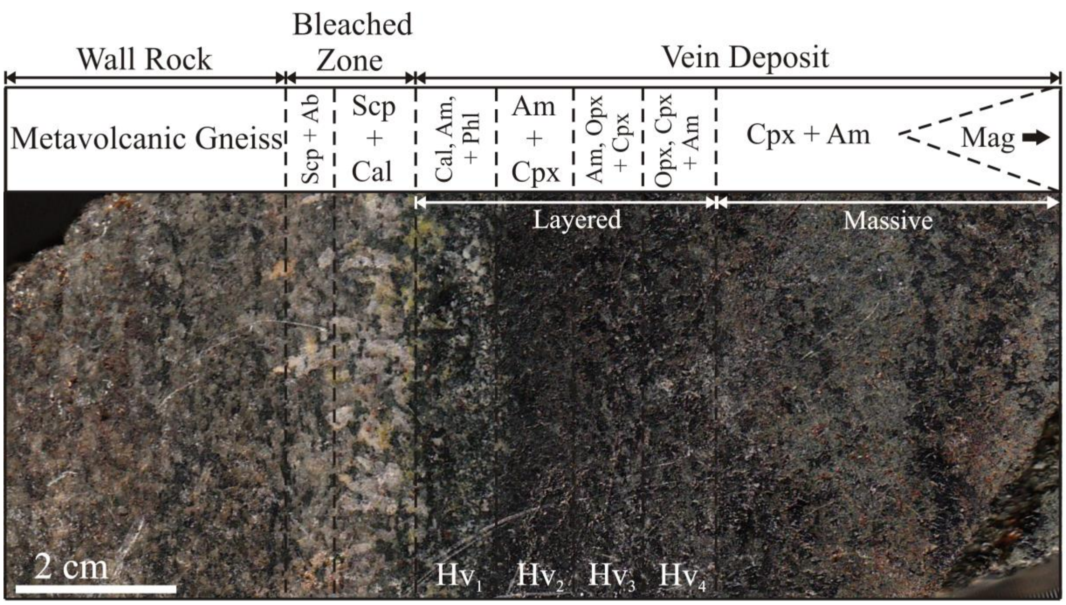


Figure 6. Sample from the Hogencamp deposit, showing banded mineral assemblages across the wall rock, bleached zone, mineralized vein contact. Layered and massive vein assemblages, and layers $Hv_1$-$Hv_4$ are also shown.

The southeastern-most shear zone contains the Hogencamp and Pine Swamp deposits. The mineralized vein that hosts both deposits is ~3 km long and ranges in thickness from 2 to 10 m at the mine locations to as little as one meter in the narrow zones that connect them. Country rock in this area includes metavolcanic and quartzofeldspathic gneiss, with diorite, calc-silicate, and marble locally.

## Hogencamp Mine

The Hogencamp deposit lies in the southern portion of the shear zone. The sheared wall rock is dominated by metavolcanic gneiss, with calc-silicate gneiss and marble locally. The vein is continuous for about one kilometer.

The bleached zone is characterized by fine-medium grained calcite (~15%) and scapolite (~15%), and the alteration of pyroxene to amphibole (~45%), with phlogopite (<10%), albite (<10%), and minor fluorapatite locally (<5%). The layered vein is composed of 'bands' of individual fine-medium grained amphibole-, clinopyroxene-, and orthopyroxene-dominated assemblages, also containing calcite and phlogopite at the bleached zone contact (Fig. 6).

Layered vein banded assemblages are designated $Hv_1$-$Hv_4$ (Fig. 6). $Hv_1$, the assemblage adjacent to the bleached zone, is composed dominantly of amphibole (~70%) and interstitial calcite (~15%) with minor clinopyroxene and (<10%) phlogopite (<5%). $Hv_2$ is mainly fine-medium grained amphibole (~60%) and clinopyroxene (~40%). $Hv_3$ is dominated by fine-medium amphibole (~45%) with lesser amounts of clinopyroxene (~35%) and orthopyroxene (~20%), whereas $Hv_4$ is dominated by medium grained orthopyroxene (~50%) and clinopyroxene (~30%) with lesser amounts of amphibole (~20%). The central massive vein is characterized by very coarse magnetite ore and coarse gangue minerals of clinopyroxene, amphibole, and biotite, cemented by interstitial calcite.

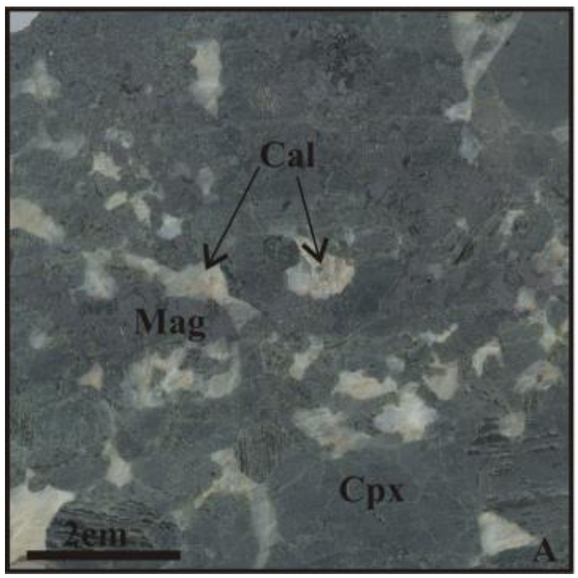


Figure 7. Massive vein from the Hogencamp deposit; clinopyroxene and magnetite with interstitial calcite.

## Pine Swamp Mine

The Pine Swamp deposit lies along strike about one kilometer northeast of the Hogencamp deposit. The vein that hosts the Pine Swamp deposit is about 500 m long, with minor semi-concordant veins in the northern extent of the deposit. This vein lies primarily in quartzofeldspathic gneiss and sulfide-bearing metavolcanic gneiss country rock, which varies between interlayered mafic and intermediate gneiss.

The bleached zone is primarily defined by retrogression of medium grained pyroxene to amphibole (~80%), but also contains minor amounts of fine-medium grained scapolite (<10%), biotite (~5%), and fluorapatite (<5%) locally. Medium-coarse grained orthopyroxene (~75%) and amphibole (~15%) dominate the narrow layered vein, with minor quartz (~10%). The massive vein contains magnetite ore and medium-coarse grained orthopyroxene (>80%) and amphibole (<20%) gangue minerals. The minerals in the massive vein are cemented by sulfide minerals, mainly pyrite and pyrrhotite. Large euhedral magnetite and sub-euhedral orthopyroxene are contained by amphibole and interstitial sulfides.

## Geochemistry

Samples were collected at each of the mines, across the wall rock-bleached zone boundary, for chemical analysis. Small, cm-scale samples were removed from the unaltered wall rock and from the bleached zone at each locality. Wall rock chemistries were averaged at each sampling location to reduce variations due to compositional heterogeneity in the cm-scale samples of gneiss (Grant, 2005). The geochemistry of the wall rock and bleached zone samples were compared to constrain elemental gains and losses into the metasomatic fluids within the zone. Grant's Isocon analysis (1987), after Gresens (1967) equation for metasomatic alteration was applied to the bulk oxide geochemistry results and density calculations. In doing so, constant alumina or titanium was assumed. The results from the isocon analysis (by percent volume change) were then used to determine the amount of each oxide gained or lost in grams per 100 grams of bulk wall rock (Δg/100g). The final mass transfer results were averaged for each of the deposits to constrain 'overall' gains and losses into the bleached zones (Table 1). Bulk rock chemistries were also acquired in cm-scale bands across layered vein material from Hogencamp Mine (Table 2). The locations of the bands are shown in Figure 6.

Average metavolcanic wall rock compositions from the Hogencamp deposit resemble an intermediate igneous rock, with 61.4% silica, 14.0% aluminum, 7.2% calcium, 6.7% iron, 4.1% potassium, and 3.6% magnesium and sodium (Table 1). The bleached zone had significant gains in calcium (6.5g), iron (~5.3g), and magnesium (2.8g), with lesser gains in titanium (~0.3g), manganese (<0.1g), and phosphorus (<0.1g), and losses in silica (3.8g), potassium (3.1g), and sodium (0.3g). On average, about 7.8 grams of material was added to the bleached zone, per 100 grams of wall rock. Averaged wall rock from the Pine Swamp deposit is similar to Hogencamp, with 63.7% silica, 14% aluminum, 7.1% iron, 6.3% calcium, 4.5% sodium, 3.2% magnesium, and 1.3% potassium. On average, the Pine Swamp bleached zone gained iron (2.4g), magnesium (~1.2g), potassium (~1.0g), and calcium (0.6g), with minor gains in titanium (~0.2g), manganese (<0.1g), and phosphorus (<0.1g), and losses in silica (~1.4g), sodium (~0.7g), and aluminum (~0.3g) per 100 grams of wall rock. An overall net gain of about 3.1 grams per 100 grams of wall rock was added to form the bleached zone (Table 1).

Table 1. Average wall rock bulk oxides and calculated mass transfer into the bleached zone.

| Oxide | Hogencamp Mine | | Pine Swamp Mine | |
|---|---|---|---|---|
| (wt%) | Wall | (Δg/100g) | Wall | (Δg/100g) |
| $SiO_2$ | 61.44 | -3.81 | 63.65 | -1.39 |
| $TiO_2$ | 0.70 | 0.28 | 0.81 | 0.19 |
| $Al_2O_3$ | 14.04 | 0.00 | 14.04 | -0.28 |
| $Fe_2O3$ | 6.66 | 5.25 | 7.10 | 2.44 |
| MnO | 0.12 | 0.07 | 0.09 | 0.01 |
| MgO | 3.58 | 2.80 | 3.23 | 1.17 |
| CaO | 7.24 | 6.50 | 6.30 | 0.62 |
| $Na_2O$ | 3.55 | -0.30 | 4.50 | -0.66 |
| $K_2O$ | 4.10 | -3.08 | 1.26 | 0.95 |
| $P_2O_5$ | 0.15 | 0.07 | 0.17 | 0.03 |
| Total | 101.57 | 7.78g | 101.16 | 3.08g |

Table 2. Bulk oxide geochemical results (in wt.%) from layered vein material.

| Oxide | Hogencamp Vein | | | |
|---|---|---|---|---|
| (wt%) | $Hv_1$ | $Hv_2$ | $Hv_3$ | $Hv_4$ |
| $SiO_2$ | 48.00 | 47.13 | 45.98 | 44.76 |
| $TiO_2$ | 0.22 | 0.32 | 0.32 | 0.32 |
| $Al_2O_3$ | 11.18 | 7.93 | 7.49 | 8.62 |
| $Fe_2O_3$ | 13.06 | 13.95 | 12.10 | 11.59 |
| MnO | 0.25 | 0.27 | 0.20 | 0.17 |
| MgO | 6.08 | 8.59 | 11.73 | 13.25 |
| CaO | 17.58 | 20.45 | 21.42 | 18.58 |
| $Na_2O$ | 1.86 | 0.91 | 0.65 | 0.91 |
| $K_2O$ | 0.67 | 0.28 | 0.50 | 1.06 |
| $P_2O_5$ | 0.49 | 0.79 | 1.30 | 1.02 |
| Total | 99.42 | 100.61 | 101.69 | 100.27 |

Bulk chemical composition of the layered vein material from Hogencamp Mine resembles that of a mafic to ultramafic igneous rock (Table 2). Silica progressively decreases from 48-44.8% into the vein, whereas magnesium increases from 6.1-13.3%. Iron shows a small net loss from 13.1-11.6%, inward whereas alumina and soda decrease progressively away from the wall and increase into the innermost analyzed layer, from 11.2-7.5% and 1.9-0.7% respectively. Potash decreases close to the wall rock from 0.7-.3%, but increases to 1.1% in the innermost layer. Similarly, calcium and phosphorus progressively increase but then decrease in the innermost layer from 17.6-21.4% down to 18.6%, and 0.5-1.3% down to 1.0%, respectively. Titanium remains relatively stable around 0.2-0.3% across all layers.

## Model of Formation

During the later stages of dextral shearing and uplift (~1,008 - 924 Ma), temperature and pressure decreases of the country rock and high fluid pressure caused the shear zones to cross the brittle-ductile transition and dilational right step-over structures formed. Country rock, still in excess of ~700°C from the waning stages of granulite facies metamorphism (~1,024 Ma), was intruded by diorites and associated pegmatites (~1,008 Ma), and later pegmatites. Acid-rich fluids derived from amphiboles and micas in metavolcanic country rock liberated iron, migrated towards the fault zones, and filled the dilational fractures.

These metamorphic fluids flushed into and filled the fractures and equilibrated with wall rocks through exchange reactions (Fig. 8A). The earliest fluids altered wall rock into bleached zone assemblages (Fig. 8B). Changes in chemistries into the bleached zone, at the wall of the vein, relative to unaltered country rock reflect the exchange of various chemical species to and from the buffered fluids. Fluid fluxes were high enough to alter wall rock to different assemblages in the bleached zone. Partially buffered to the composition of local country rocks, these fluids were transported and mixed along strike during seismically induced pumping events, dilating the structures further. The fluids encountered and mixed with fluids from other sections of the fault and changed in composition, finding favorable physical and/or chemical conditions for mineralization within the dilational areas in the fault zones (Fig. 8C).

Pressure drops and fluid mixing at the dilational segments of the faults caused certain species in the fluids to become supersaturated and prompted precipitation. Minerals precipitated in the confined cracks, and resulted in the early layered vein deposits, primarily composed of alternating pyroxene- and amphibole-rich assemblages (Fig. 8C). Nucleation sites were primarily along the walls, and only allowed for fine- to medium-grained crystal growth. The layered vein assemblages provide mineralogical, textural, and geochemical evidence for seismic pumping and the local mixing of fluids, and REE concentrations are evidence of regionally closed system behavior (Kalczynski and Gates, 2014). By the time the first layer of vein assemblages was deposited in the vein fractures, bleached zone forming exchange reactions ceased, as the fluids were no longer in contact with original wall rock, and country rock temperature and fluid pH no longer permitted exchange reactions to occur.

The buffered fluids contributed to layered vein assemblages, as they mixed and flushed along the fault zones. In areas of calc-silicate country rock (Hogencamp deposit), abundant calcium was mobilized into the fluids and resulted in calcium-rich vein assemblages, dominated by clinopyroxene, calcite, amphibole, scapolite, and minor micas (Fig. 9). In quartzofeldspathic and metavolcanic country rock (Pine Swamp deposit), silica was abundant, and most mobilized during mass transfer and vein deposition. Silica-enriched assemblages are dominated by amphibole, orthopyroxene, scapolite, quartz, and/or sulfides.

With continued dilation, large fluid volumes were introduced to and trapped in larger cavities, and the dominant mode of mineralization favored massive deposits (Fig. 8D). Mineralization along the faults eventually sealed fluids in the fault zones and dilational segments as the system became closed, even at the local level. Fluids became iron and volatile-rich as other chemical species were depleted through crystallization. Fluid ratios increased, depressing crystal nucleation sites and aiding in element mobility allowing massive magnetite and ferromagnesian-rich assemblages, including euhedral crystals, to form in these cavities (Fig. 8D). Fluid pressure in these large cavities was also lower than surrounding country rock, dropping the solubility of iron and prompting mineralization. Mixing of carbonate-rich fluids neutralized the acidic fluids, also lowering the solubility of magnetite, further promoting precipitation. Temperature and pressure decreases limited the crystallization reactions, dominantly mineralizing magnetite and the few other gangue minerals.

As chemical species were depleted crystallizing the massive gangue minerals, the remaining dissolved iron oxidized and was deposited as the massive magnetite bodies. Locally buffered fluids also contributed to the gangue minerals of the massive assemblages. Clinopyroxene and interstitial calcite formed in deposits near calc-silicate and marble (Hogencamp), and orthopyroxene/amphibole and interstitial quartz and/or pyrite formed in deposits near quartzofeldspathic and metavolcanic country rock (Pine Swamp). Late in the massive vein mineralization process the interstitial minerals (calcite, quartz, and sulfides) overprinted the massive assemblages (see Kalczynski and Gates, 2014).

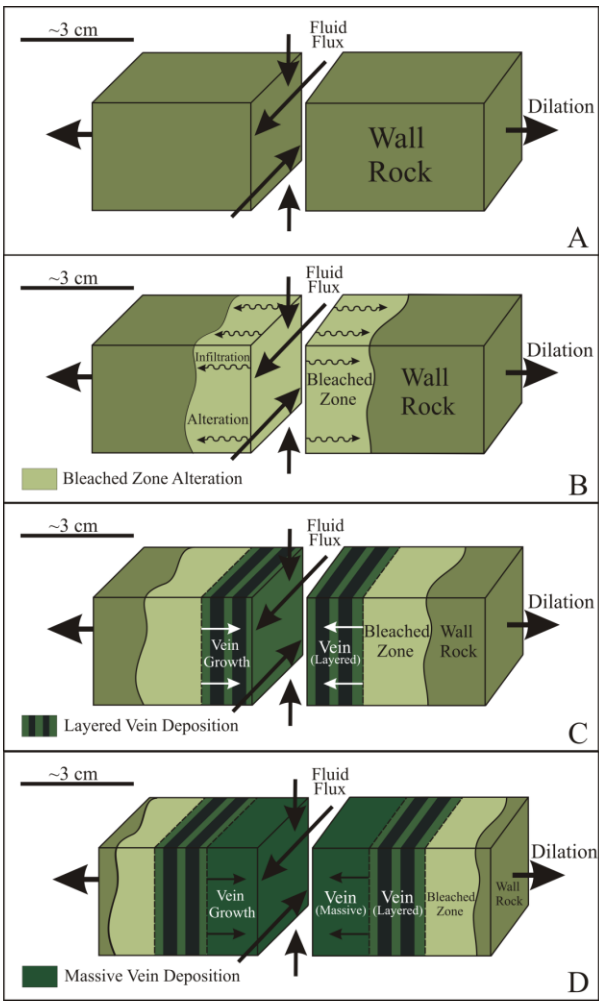


Figure 8. Schematic block model of the formation of the vein deposits. (modified after Weisenberger and Bucher, 2010).

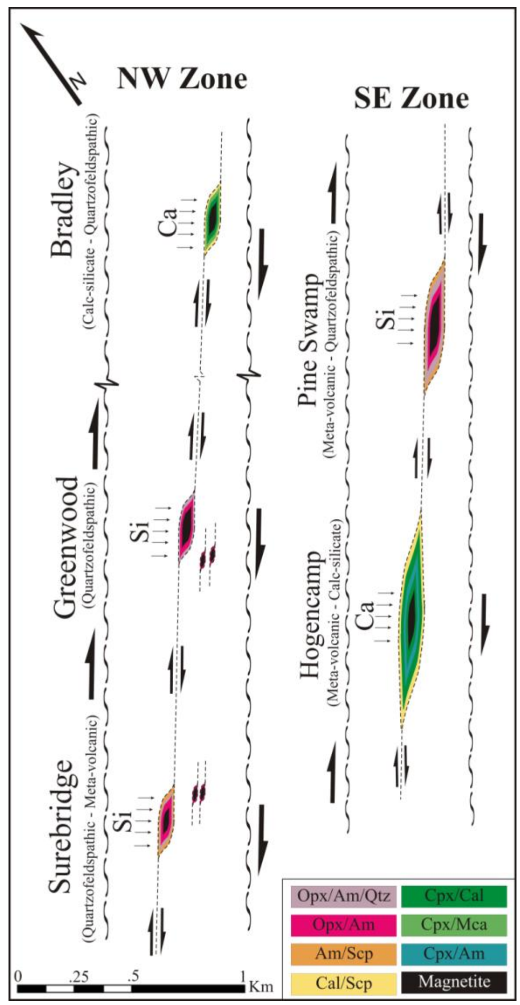


Figure 9. Schematic diagram of the vein deposit's dominate mineral assemblages, and sources of some chemical species.

# LATE PROTEROZOIC TECTONIC HISTORY

A volcanic pile formed about 1.2 Ga in an island arc or marine magmatic arc setting characterized by layered intermediate and mafic rocks, and associated plutons and volcaniclastic sediments (Gates *et al.*, 2001). This sequence underwent granulite facies metamorphism, about 1,050 Ma associated with the Ottawan phase of the Grenville orogeny (Gates *et al.*, 2003). Locally, anatexis produced migmatites, granite sheets, and the early pegmatites (Gates *et al.*, 2003). The Ramapo and Reservoir fault zones were activated as ductile reverse faults. Subsequent diorite intrusions occurred around 1,008 Ma, either the result of delamination at the end of the first event, or the early dilational stages of the next event (Gates *et al.*, 2003). This second event is characterized by dextral strike-slip movement during a period of rapid uplift and unroofing at approximately 1,008 Ma to 924 Ma (Gates and Krol, 1998). Thick anastomosing zones of mylonite formed, overprinting previous features. Offset reached upwards of 100's of kilometers (Gates *et al.*, 2003). Both Ramapo and Reservoir fault zones were reactivated as ductile dextral strike-slip faults. Strike-slip shearing continued during rapidly decreasing temperatures, resulting in smaller, local shear zones crossing the brittle-ductile transition and becoming dilational (Gates *et al.*, 2003). Regionally derived, but locally chemically buffered fluids resulted in the mineralization of magnetite vein assemblages in dilational shear zones. The vein assemblages reflect the changing chemistries of the fluids from changes in flux, fluid buffering source, chemical, and/or physical conditions (Kalczynski and Gates, 2014).

# CONCLUSIONS

The Grenville event in the New Jersey and Hudson Highlands of the central Appalachians was formed in a fourfold tectonic scenario (Gates *et al.*, 2003).

1. Deposition of volcanic and volcaniclastic sediment within a subduction zone complex ca 1.2 Ga.
2. Continental collision of the arc with another continent to the east during the building of the Rodinian supercontinent occurred at ca. 1,050-1,020 Ma. Granulite facies metamorphism and extensive pegmatite intrusion accompanied this event.
3. After orogenesis ceased, dioritic melts intruded the area, ca. 1,008 Ma., accompanying period of extension or mantle delamination.
4. Strike-slip shearing resulting from tectonic escape probably lasted from 1,008-980 Ma or later. There was a rapid decrease in temperature during this event resulting in the shear zones crossing the brittle-ductile transition and becoming dilational. Extensive mineralization occurred within these dilational fractures.

Meeting Point: West parking lot of the Double Tree Inn, located at 425 NY-59, Nanuet, NY, 10954.

Meeting Point Coordinates: 18T 0584372mE, 4549264mN

Meeting Time: 8:30 AM

| Distance in Miles (km) Cumulative | Point to Point | Route Description |
|---|---|---|
| **0.0 (0.0)** | 0.0 (0.0) | Assemble in the western parking lot of the Double Tree Inn in Nanuet, NY. |
| **0.3 (0.5)** | 0.3 (0.5) | Head East on NY-59 E toward Rose Rd. |
| **0.5 (0.8)** | 0.2 (0.3) | Use the right lane to take the ramp to Palisades County Rd N. |
| **9.9 (15.9)** | 9.4 (15.1) | Merge onto Palisades Interstate Parkway N. |
| **10.1 (16.3)** | 0.2 (0.3) | Take exit 14 for Willow Grove Rd toward Letchworth Village. |
| **11.6 (18.7)** | 1.5 (2.4) | Turn left onto Willow Grove Rd. |
| **15.1 (24.3)** | 3.5 (5.6) | Merge onto Kanawauke Rd. |
| **15.4 (24.8)** | 0.3 (0.5) | At the Kanawauke traffic circle, take the second exit and stay on Kanawauke Rd (Route 106). |
| **16.0 (25.7)** | 0.6 (1.0) | Continue on Kanawauke Rd for 0.6 miles until reaching the bridge over the eastern-most extent of Little Long Pond. If needed, parking can be found a quarter mile east on Kanawauke Rd at the picnic area (lavatory facilities). Walk 100 feet to the north-west on Kanawauke Rd to the first road-cut (Stop 1, Fig. 11). |

STOP 1: Unsheared Metavolcanic Gneiss, Harriman State Park, NY

Location Coordinates: 18T 0573484mE, 4565104mN

Strongly interlayered intermediate and mafic gneisses with migmatitic bodies, just outside of the SE shear zone. Mafic layers are characterized by assemblages of clinopyroxene and amphibole with minor plagioclase, magnetite, sphene, and apatite. Intermediate layers are mainly plagioclase with minor quartz, apatite, amphibole, and biotite. The felsic leucosome is composed of coarse plagioclase, quartz, and K-feldspar, which form veins and clots including classic “net veining”. Minerals exhibit preferred orientations in the gneiss and appear granular in the leucosome. Late stage K-feldspar pegmatites can also be observed in this outcrop, containing mafic gneiss xenoliths.

Gneisses exhibit a strongly banded, intermediately dipping, foliation that strikes N-NE. Isoclinal intrafolial folds can also be observed, with axis following similar orientation. This deformation is indicative of main stage Grenville tectonism, and was unaffected during the later tectonic event, associated with the formation of the ore deposits. Contrast these rocks with Stop 2.

| Distance in Miles (km) Cumulative | Point to Point | Route Description |
|---|---|---|
| **16.0 (25.7)** | 0.0 (0.0) | Head west on route 106 for roughly 600 feet to the large peninsula protruding into Little Long Pond. Proceed 250 feet to the south to reach the tip of the peninsula (Stop 2, Fig. 12). |

STOP 2: Southeastern Shear Zone Boundary, Harriman State Park, NY

Location Coordinates: 18T 0573272mE, 4565124mN

Several meter scale lozenge and cigar shaped boudins of mafic gneiss are contained within mylonitic quartzofeldspathic gneiss, with folded biotite and local amphibole-rich layers. The layers appear contorted and wrap around the mafic bodies. The encased mafic gneiss is similar to that of Stop 1, however it also contains contorted folds and veins of magnetite. The long axis of the bodies and fold axis appear sub-parallel, and shallowly plunge to the northeast.

Both Stops 1 and 2 are similar in composition and therefore grouped within the same metavolcanic sequence. Long axis and fold axes roughly parallel shear zone boundaries and fabrics within. This location is at the edge of the southeastern dextral, strike-slip shear zone. Deformation steadily increases to the northwest, into the central shear zone, characterized by a steepening of planar fabric and increase in intensity of linear fabric. The contrast of the features at Stop 1 with Stop 2 shows the difference between the first main Grenville and second strike-slip events.

| **Distance in Miles (km)** | | **Route Description** |
|---|---|---|
| **Cumulative** | **Point to Point** | |
| **16.0 (25.7)** | 0.0 (0.0) | Locate the gated path directly on the opposite side of Kanawauke Rd. Walk this path heading north for a quarter mile, to the intersection with Dunning Trail (E-W trending). Head roughly northeast on Dunning Trail for about a half mile until you reach several large holes in the ground, and the path crosses a small stream. Hike upstream for roughly 100 feet until you are almost cliff side. A linear open pit mine should be visible to the southwest and a large mine shaft to the northeast into the cliff, beneath Cape Horn (Stop 3, Fig. 13). |

STOP 3: Hogencamp Mine, Harriman State Park, NY

Location Coordinates: 18T 0573790mE, 4566280mN

Hogencamp Mine lies in the southern part of the mineralized zone. Here the sheared wall rock is dominated by quartzofeldspathic and amphibole-pyroxene (metavolcanic) gneisses with interlayered calc-silicate gneiss and marble locally. Hogencamp Mine was active from the earliest to latest 18$^{th}$ century. It is characterized by a series of meter to several meter scale horizontal and vertical mine shafts and open pit mines. The mines can be traced along strike for up to a kilometer. The mineralized zone that hosts Hogencamp Mine is roughly 6 kilometers long and extends into Pine Swamp Mine (Stop 4). The vein ranges in thickness from 3 to 15 meters at the mine locations to as little as one meter in the narrow zones connecting the deposits. The Hogencamp Mines can be followed to the southwest from this location for up to a kilometer.

The vein-wall rock contact is sharp and semi-concordant to mylonitic foliation. On the small-scale it appears slightly discordant, crosses foliation and erodes into the wall rock. This is best observed in the open pit mine, directly in front of the northeastern most mine shaft, below Cape Horn (Fig. 10). Here, the bleached zone is characterized by the deposition of calcite and scapolite, and retrogression pyroxene to amphibole, also containing phlogopite, calcite, and minor apatite locally. Earliest vein deposit is characterized by layered amphibole, orthopyroxene, and clinopyroxene, later by massive clinopyroxene and magnetite, cemented by late stage, interstitial calcite in the ore zone. Clinopyroxene and localized magnetite are euhedral, forming doubly terminated crystals, thought to have crystallized in cavities. The veins are also intruded by very coarse grained pegmatites which contain xenoliths of the mafic vein material.

Figure 10. Hogencamp (Stop 3, left) and Pine Swamp (Stop 4, right) Mines.

| Distance in Miles (km) Cumulative | Point to Point | Route Description |
|---|---|---|
| **16.0 (25.7)** | 0.0 (0.0) | Back on Dunning Trail, walk east than north-northeast, another half mile until you reach a large swamp to the east, and a large, steep hillside to the west, littered with dark-colored mine tailings. Locate the makeshift path on the hillside. Take this path uphill for about two hundred feet, until your reach the entrance to the mine (Stop 4, Fig. 13). |

STOP 4: Pine Swamp Mine, Harriman State Park, NY

Location Coordinates: 18T 0574253mE, 4566795mN

Pine Swamp Mine lies in the northern part of the shear zone within the same mineralized vein which hosts Hogencamp Mine, roughly one kilometer alone strike (NE). Pine Swamp is also characterized by a 3 to 12 meter horizontal mine openings and several, meter scale open pit mines (Fig. 10). The mines that compromise the Pine Swamp deposit can be traced along strike for several hundred meters, with minor semi-concordant offshoots in the northern extent of the deposit. This portion of the hydrothermal vein lies dominantly within sulfide-bearing quartzofeldspathic gneiss country rock, which contains interlayered metavolcanic gneisses. The bleached zone is primarily defined by retrogression of pyroxene to amphibole, also containing minor amounts of scapolite, and apatite locally. Orthopyroxene and amphibole dominate the narrow layered vein and thick massive sequences followed by the magnetite deposits. Massive minerals are locally cemented by late stage sulfide minerals, mainly pyrite and pyrrhotite. The flat wall adjacent to the mine proper is yellow to rust colored, due to the weathering of the sulfide-rich country rock. Massive minerals orthopyroxene, amphibole, and substantial magnetite can also be observed.

| Distance in Miles (km) Cumulative | Point to Point | Route Description |
|---|---|---|
| **16.0 (25.7)** | 0.0 (0.0) | Take Dunning Trail south and west back to the first intersection of paths. Head south on the first path, to exit back at the gated entrance. |
| **16.7 (26.9)** | 0.7 (1.1) | Drive east on Kanawauke Rd to Kanawauke Circle, and take the third exit to head north on Seven Lakes Drive. |
| **19.1 (30.7)** | 2.4 (3.9) | Continue north on Seven Lakes Drive until reaching Lake Tiorati. Stop 5 is a large road cut, ~650 feet north of Cedar Pond Rd, on the left (west) side of the Seven Lakes Drive. Please park vehicles as far on the shoulder closest to the lake as possible. Lavatory facilities and additional parking can be found ~3/4 of a mile north on Seven Lakes Drive at Tiorati Circle. |

STOP 5: Lake Tiorati Diorite, Harriman State Park, NY

Location Coordinates: 18T 0575665mE, 4568681mN

Pluton of coarse- to very coarse grained black and white speckled diorite. On the south side of the outcrop, the diorite is equigranular in texture with random grain orientation. It contains a roof pendant of well-foliated biotite quartzofeldspathic gneiss that exhibits crenulation cleavage. The xenolith contains a drag fold along its contact with the diorite. It also contains a rim of granitic pegmatite that connects to pegmatite and quartz veins within the diorite. The diorite contains plagioclase and hornblende and clinopyroxene but with brown cores or orthopyroxene. Other phases include magnetite and ilmenite. In the northern part of the exposure, the diorite is crossed by anastomosing mylonite bands. The mylonite strikes northeast and is near vertical. Lineations plunge shallowly to the northeast. Kinematic indicators include rotated porphyroclasts and S-C fabric. Where it can be determined, shear sense is consistently dextral.

Subsequent to the first tectonic event which included the nappe emplacement and granulite facies metamorphism, there was a period of intermediate plutonism. The xenolith was deformed and metamorphosed prior to intrusion. The xenolith became more ductile as a result of the heat of the pluton. Thus, drag folds formed along its edges as it fell into the magma. The magma was hot enough to cause partial melting of the rim of the xenolith, producing a granitic melt. The diorite crystallized at a higher temperature than the granitic melt. Fractures opened in the newly crystallized rock and the remaining granitic melt squeezed into them forming the veins. Later deformation produced the mylonitic fabric in the diorite. This outcrop is at the eastern edge of a large dextral strike-slip shear zone with similar orientation.

| Distance in Miles (km) Cumulative | Point to Point | Route Description |
|---|---|---|
| **21.6 (34.8)** | 2.5 (4.0) | Turn around on Seven Lakes Drive to head southbound. |
| **26.7 (43.0)** | 5.1 (8.2) | At the Kanawauke Circle, take the first exit onto Kanawauke Rd (Route 106). |
| **27.6 (44.4)** | 0.9 (1.4) | Continue onto NY-17A westbound. Stop 6 is a large road cut on the northern (right) side of 17A. Park on the shoulder of the road, and proceed onto the outcrop. |

STOP 6: 17A Indian Hill Mylonite Zone, Tuxedo, NY

Location Coordinates: 18T 0567611mE, 4565080mN

The rock is biotite quartzofeldspathic mylonite gneiss with interlayers of biotite gneiss locally, interpreted to have a volcaniclastic origin. The mylonite is well foliated and lineated and composed of plagioclase, quartz, potassium feldspar, and biotite. This mylonite exhibits well developed kinematic indicators including S-C fabric, reverse shear cleavage (RSC), rotated porphyroclasts, and shear bands. These kinematic indicators show a consistent dextral shear sense. The width of the zone and the low S-C angle indicate significant offset during the second event. Because this shear zone developed in biotite-rich gneiss, it displays kinematic indicators better than most zones. It is another in the series of anastomosing dextral shear zones that were produced during the second event. The gneiss is interpreted to have a volcaniclastic origin.

| **Distance in Miles (km)**<br>**Cumulative** | **Point to Point** | **Route Description** |
|---|---|---|
| **28.1 (45.2)** | 0.5 (0.8) | Head West on NY-17A W toward Clinton Rd. |
| **29.5 (47.5)** | 1.4 (2.3) | Make a U-turn at Clinton Rd. |
| **36.5 (58.7)** | 7 (11.3) | Turn right to merge onto NY-17 S. |
| **36.8 (59.2)** | 0.3 (0.5) | Use the right lane to take the NY-17 S/Interstate 87 S/New York Thruway ramp to Interstate 287. |
| **37.8 (60.8)** | 1 (1.6) | Merge onto I-87 S/NY-17 S. |
| **38.6 (62.1)** | 0.8 (1.3) | Use the right lane to take exit 15 for NY-17 S/I-287 S toward New Jersey. |
| **39.2 (63.1)** | 0.6 (1.0) | Continue onto I-287 S (entering New Jersey). |
| **52.7 (84.8)** | 13.5 (21.7) | Keep Right to stay on I-287 S. |
| **52.8 (85.0)** | 0.1 (0.2) | Take exit 52A-52B for NJ-23 toward Riverdale/Wayne/Butler. |
| **53.1 (85.5)** | 0.3 (0.5) | Keep left at the fork, follow signs for State Highway 23 and merge onto NJ-23 S/State Highway 23 S. |
| **53.7 (86.4)** | 0.6 (1.0) | Merge onto NJ-23 S/State Highway 23 S. |
| **53.7 (86.4)** | 0 (0) | Slight right onto West Parkway. |
| **54.2 (87.2)** | 0.5 (0.8) | Turn right onto West Parkway. Stop 7 is located in a small (Foot Hill) park on the right (northwest) side of West Parkway, closest to I-287. Park in the parking lot and proceed to the outcrop ~100 feet to the west of the parking lot. |

Figure 11. Stop 7. Outcrop of Ramapo fault zone, located in Riverdale, NJ.

STOP 7: Ramapo Fault Zone, Riverdale, NJ

Location Coordinates: 18T 0557739mE, 4536780mN

The northeast-trending Ramapo fault zone is the major border fault which juxtaposes the Proterozoic gneisses of the New Jersey Highlands with the Mesozoic sedimentary and igneous rocks of the Newark Basin. Width of the fault zone varies from approximately 5 to 10 km (Ratcliffe, 1980). Abundant moderate to steep southeast-dipping zones up to 25 m thick are developed within the granitic gneisses of the fault zone and exhibit mesoscopic S-C mylonite fabric. The fault zone is also intruded by mafic dikes which have been subsequently sheared during brittle reactivation. The Ramapo fault zone originally developed as a reverse right-lateral strike-slip fault during the Grenville orogeny (Ratcliffe, 1980) and has a long and complex kinematic history which included four to five recognizable episodes of fault movement. Despite the long history of reactivation of the zone there is no strong evidence of any post-Mesozoic or neotectonic movement. The mylonites within the Ramapo fault zone consistently indicate top to the northwest reverse faulting. These zones were reactivated under mid- to upper-greenschist facies conditions during the Taconic orogeny approximately 450 to 460 Ma (Ratcliffe, 1980) (Costa and Gates, 1993).

This exposure is located in Foot Hill Park at the end of West Parkway in Riverdale, New Jersey (Fig. 11). The entire exposure consists of ultramylonite of the Ramapo fault zone. Glacial striations oriented essentially north-south have polished the surface of the exposure. The alternating black and white/gray bands of foliation dip moderately to the southeast. The black bands are composed of fine-grained foliated chlorite, whereas the white/gray bands are quartzofeldspathic. Both quartz and feldspar deformed in a ductile manner, and are extensively dynamically recrystallized. Small grains of pyrite are present within the foliation.

| Distance in Miles (km) Cumulative | Point to Point | Route Description |
|---|---|---|
| **54.2 (87.2)** | 0 (0) | Head north on West Parkway (left out of the Foot Hill Park parking lot). |
| **54.7 (88.0)** | 0.5 (0.8) | Keep Left to continue onto Boulevard. |
| **57.6 (92.7)** | 2.9 (4.7) | Use any lane to turn left at the 1st cross street onto NJ-23 N. |
| **68.1 (109.6)** | 10.5 (16.9) | Continue on NJ-23 N. |
| **68.1 (109.6)** | 0 (0) | Slight right toward Canistear Rd. |
| **68.2 (109.8)** | 0.1 (0.2) | Turn left onto Canistear Rd. |
| **68.2 (109.8)** | 0 (0) | Turn left at the 1st cross street onto NJ-23 S/Paterson Hamburg Turnpike S. |
| **68.7 (110.6)** | 0.5 (0.8) | Continue on NJ-23 S for half a mile. Park on the right hand shoulder (west side) of NJ-23 S, just before the road-side barrier and the shoulder narrows. Walk down the hill and cross the stream at the narrow portion. Continue to walk southbound along the western edge of Oak Ridge Reservoir for ~half a mile. The exposures are just around the bend of the reservoir, at the reservoirs edge, facing southward. |

STOP 8: Reservoir Fault Zone, West Milford, NJ

Location Coordinates: 18T 0542826mE, 4546228mN

This stop illustrates how hydrothermal chemical and resulting mineralogical changes in a fault zone can change deformation style from brittle to ductile. We will observe undeformed protolith (granitic gneiss), hydrothermally mineralized cataclasite (brittle), and mylonite (ductile) of the mineralized zone. The undeformed to slightly deformed rock is mapped as pyroxene gneiss and interpreted as a metasedimentary sequence. The rock consists of diopside-, amphibole- and rarely scapolite-bearing granitic to quartz dioritic gneiss with sparse interlayered amphibolite gneiss and pegmatite veins. The faulted rocks are cataclasite and breccia with mainly rounded blocks and clasts of granitic-quartz dioritic gneiss.

The matrix material is composed of ~95% randomly oriented actinolite with minor epidote, albite, chlorite, and sulfides although finely ground xenocrystic phases from the gneiss are locally abundant. Thin ductile shear zones can be found in this outcrop but the structures observed are primarily the result of brittle deformation coupled with hydrothermal activity that produced the amphibole-sulfide mineralization. After formation through hydrothermal alteration, the amphibole-rich matrix underwent ductile deformation forming an S-C mylonite, more typical of rocks found in the center of the fault zone. The ductile deformation produced a strong foliation with significantly reduced grain size. Kinematic indicators include dragged foliation, S and C bands, rotated porphyroclasts, and offset markers showing a consistent dextral strike-slip sense (Gates, 1993).

| **Distance in Miles (km)** | | **Route Description** |
|---|---|---|
| **Cumulative** | **Point to Point** | |
| **68.7 (110.6)** | 0 (0) | Back-track to return to the road side and vehicles. |
| **81.1 (130.5)** | 12.4 (20.0) | Head south on NJ-23 S. |
| **81.4 (131.0)** | 0.3 (0.5) | Use the right lane to merge onto I-287 N via the ramp to Mahwah. |
| **81.4 (131.0)** | 0 (0) | Merge onto I-287 N. |
| **88.0 (141.6)** | 6.6 (10.6) | Keep left to stay on I-287 N (entering New York). |
| **96.0 (154.5)** | 8 (12.9) | Use the right 2 lanes to merge onto I-287 E/I-87 S toward Tappan Zee Bridge/New York City. |
| **103.7 (166.9)** | 7.7 (12.4) | Take exit 14 for NY-59 toward Spring Valley/Nanuet. |
| **103.9 (167.2)** | 0.2 (0.3) | Use the left 2 lanes to turn left onto NY-59 E. |
| **105.6 (169.9)** | 1.7 (2.7) | Return to Double Tree Inn at 425 New York 59, Nanuet, NY, 10954. Destination will be on the right. |
| | | ***END TRIP*** |

## REFERENCES CITED

Bartholomew, M.J. and Lewis, S.E., 1988, Peregrination of Middle Proterozoic massifs and terranes within the Appalachian orogen, eastern U.S.A.: Trabajos de Geologia, v. 17, p. 155-165.

Beach, A., 1975, The geometry of en-echelon vein arrays: Tectonophysics, v. 28, p. 245-263.

Boullier, A.M. and Bouchez, J.-L., 1978, Le quartz en rubans dans las mylonites: Bull. Soc. Geol. Fr., v. 20, p. 253-262.

Costa, R.E., 1991, Structural evolution and neotectonics of the Ramapo fault system, northern New Jersey: Dept. of Geological Sciences, Rutgers University, Newark, unpublished Master's thesis, 83 p.

Costa, R. and Gates, A.E., 1993, Multiple episodes of movement on the Ramapo fault system, northern New Jersey, *in* Puffer, J.H. (ed.), Geologic Traverse across the Precambrian Rocks of the New Jersey Highlands: Geological Association of New Jersey Field Guide and Proceedings, v. 10, p. 168-195.

Dallmeyer, R.D., 1974, Metamorphic history of the northeastern Reading Prong, New York and Northern New Jersey: Journal of Structural Geology, v. 15, p. 325-359.

Drake, A.A. Jr., 1984, The Reading Prong of New Jersey and eastern Pennsylvania, An appraisal of rock relations and chemistry of a major Proterozoic terrane in the Appalachians, *In* Bartholomew, M.J. (ed.), The Grenville Event in the Appalachians and Related Topics, Geological Society of America Special Paper 194, p. 94-109.

Dodd, R.T. Jr., 1965, Precambrian geology of the Popolopen Lake quadrangle, southeastern New York: New York State Museum and Science Service Map and Chart Series, No. 6, 39 p.

Eisbacher, G.H., 1970, Deformation mechanisms of mylonite rocks and fractured granulites in Cobequid Mountains, Nova Scotia, Canada: Geological Association of America Bulletin, v. 81, p. 2009-2020.

Eugster, H.P., 1986, Minerals in hot water: American Mineralogist, v. 71, p. 655-673.

Finks, R.M., 1990, The Green Pond outlier as a Silurian right-lateral transpressional basin: Geological Society of America, Abstracts with Programs, v. 22, p. 15.

Gates, A.E., 1993, Chemical changes in mylonites and cataclasites of the Reservoir fault zone, New Jersey, *in* Puffer, J.H. (ed.) Geologic Traverse across the Precambrian Rocks of the New Jersey Highlands, Geological Association of New Jersey Field Guide and Proceedings, v. 10, p. 148-167.

Gates, A.E., 1995, Middle Proterozoic dextral strike-slip event in the central Appalachians- Evidence from the Reservoir fault, NJ: Journal of Geodynamics, v. 19, p. 195-212.

Gates, A.E., 1998, Early compression and late dextral transpression within the Grenvillian Event of the Hudson Highlands, NY, USA, *in* Sinha, A.K. (ed.), Basement Tectonics 13; Dordrecht, The Netherlands, Kluwer Academic Publishers, p. 85-98.

Gates, A.E., and Costa, R.E., 1998, Multiple reactivations of rigid basement block margins: Examples in the northern Reading Prong, USA, *in* Gilbert, M. C. and Hogan, J.P. (eds.), Basement Tectonics 12: Central North America and Other Regions; Dordrecht, The Netherlands, Kluwer Academic Publishers, p. 123-153.

Gates, A.E. and Krol, M.A., 1998, Kinematics and thermochronology of late Grenville escape tectonics from the central Appalachians: Geological Society of America, Abstracts with Programs, v. 30.

Gates, A.E., Valentino, D.W., Gorring, M.L., Chiarenzelli, J.R., and Hamilton, M.A., 2001, Bedrock geology, geochemistry and geochronology of the Grenville Province in the western Hudson Highlands, New York, *In* Gates, A.E. (ed.), Geology of the Lower Hudson Valley: New York State Geological Association Guidebook, p. 177–204.

Gates, A.E., Valentino, D.W., Chiarenzelli, J., Gorring, M., and Hamilton, M., 2003, Field Trip to the Western Hudson Highlands: 2003 Long Island Geologists Conference, 30 p.

Gates, A.E., Valentino, D.W., Chiarenzelli, J.R., Solar, G.S., and Hamilton, M.A., 2004, Exhumed Himalayan-type syntaxis in the Grenville Orogen, northeastern Laurentia: Journal of Geodynamics, v. 37, p. 337–359.

Gates, A.E., Valentino, D.W., Gorring, M., Thern, E.R., and Chiarenzelli, J.R., 2006, Rodinian collisional and escape tectonics in the Hudson Highlands, New York, *In* Pazzaglia, F.J. (ed.), Excursions in Geology and History: Field Trips in the Middle Atlantic States, Geological Society of America Field Guide 8, p. 65-82.

Grant, J.A., 1986, The isocon diagram—a simple solution to Gresens' equation for metasomatic alteration: Economic Geology, v. 81, p. 1976–1982.

Grant, J.A., 2005, Isocon analysis: A brief review of the method and applications: Physics and Chemistry of the Earth, v. 30, p. 997-1004.

Gresens, R.L., 1967, Composition–volume relationships of metasomatism: Chem. Geol., v. 2, p. 47–55.

Gundersen, L.C.S., 1986, Geology and geochemistry of the Precambrian rocks of the Reading Prong, New York and New Jersey - Implications for the genesis of iron-uranium-rare earth deposits, *In* Carter, L.M.H. (ed.), USGS Research on Energy Resources -1986 Programs and Abstracts, US Geological Survey Circular, v. 974, p. 19.

Gundersen, L.C.S., 2004, Tectonics and metallogenesis of Proterozoic rocks of the Reading Prong: Journal of Geodynamics, v. 37, p. 361-379.

Hague, J.M., Baum, J.L., Hermann, L.A., and Pickering, R.J., 1956, Geology and structure of the Franklin-Sterling area, New Jersey: Geological Society of America Bulletin, v. 68, p. 435-473.

Harding, T.P., 1974, Petroleum traps associated with wrench faults: American Association of Petroleum Geologists Bulletin, v. 58, p. 1290-1304.

Helenek, H.L., 1971, An investigation of the origin, structure and metamorphic evolution of major rock units in the Hudson Highlands: PhD Thesis, Brown University.

Herman, G.C. and Mitchell, J.P., 1991, Bedrock geologic map of the Green Pond Mountain region from Dover to Greenwood Lake, New Jersey: New Jersey Geological Survey, Geologic Map Series 91-2.

Hippert, J.F.M., 1993, 'V'-pull-apart microstructures: a new shear sense indicator: Journal of Structural Geology, v. 15, p. 1393-1403.

Hull, J., Koto, R., and Bizub, R., 1986, Deformation zones in the Highlands of New Jersey, *in* Husch, J.M. and Goldstein, F.R., (eds.), Geology of the New Jersey Highlands and Radon in New Jersey, Geological Association of New Jersey Field Guide, v. 3, p. 19-67.

Kalczynski, M.J. and Gates, A.E., 2014, Hydrothermal alteration, mass transfer, and magnetite mineralization in dextral shear zones, western Hudson Highlands, New York, United States. *Ore Geology Reviews* v. 61, p. 226-247.

Krol, M.A., Gosse, J., Hedlund, C., Messina, T., Tenore-Nortrup, J., Winslow, D., and Zeitler, P., 1992, 40Ar/39Ar constraints in the extent of both Paleozoic and and Mesozoic thermal overprinting of Reading Prong basement adjacent to the Newark basin, EOS Transactions, American Geophysical Union Abstracts with Programs, v. 73, p. 279.

Krol, M.A. and Zeitler, P.K., 1994, 40Ar/39Ar constraints on regional thermal resetting of alkali feldspars from the Newark basin and adjacent Reading Prong, Eighth International Conference on Geochronology, Cosmochronology and Isotope Geology, U.S. Geological Survey Circular, v. 1107, p. 180.

Lister, G.S. and Snoke, A.W., 1984, S-C mylonites: Journal of Structural Geology, v. 6, p. 617-638.

Lewis, J.V. and Kummel, H.B., 1912, Geologic map of New Jersey (1910-1912), New Jersey Dept. of Conservation and Economic Development, Atlas Sheet 20.

Lupulescu, M. and Gates, A.E., 2006, Iron deposits from Hudson Highlands, NY: Systematics, mineralogy, mineral chemistry and tectonic setting: Geological Association of New Jersey Field Guide and Proceedings, v. 23, p. 46-59.

Malizzi, L. D. and Gates, A. E., 1989, Late Paleozoic deformation in the Reservoir Fault zone and Green Pond Outlier: N. Y. State Geological Assoc. Field Trip Guidebook, v. 61, p. 75-93.

Mitchell, J.P. and Forsythe, R., 1988, Late Paleozoic non-coaxial deformation in the Green Pond outlier, New Jersey Highlands: Geological Society of America Bulletin, v. 100, p. 45-59.

Olsen, P.E., 1980, Triassic and Jurassic formations of the Newark basin, in (Manspeizer, W. eds) Field studies of New Jersey Geology, New York State Geological Association Guidebook, v. 52, p. 1-39.

Passchier, C.W. and Simpson, C., 1986, Porphyroclast systems as kinematic indicators: Journal of Structural Geology, v. 8, p. 831-843.

Petit, J.P., 1987, Criteria for the sense of movement on fault surfaces in brittle rocks: Journal of Structural Geology, v. 9, p. 597-608.

Puffer, J.H. and Gorring, M.L., 2005, The Edison magnetite deposits in the context of pre-, syn-, and post-orogenic metallogenesis in the Grenville Highlands of New Jersey: Canadian Journal of Earth Sciences, v. 42, p. 1735-1748.

Ratcliffe, N.M., Armstrong, R.L., Chai, B.H., and Senechal, R.G., 1972, K-Ar and Rb-Sr geochronology of the Canopus pluton, Hudson Highlands, New York: Geological Society of America Bulletin, v. 83, p. 523-530.

Ratcliffe, N.M., 1980, Brittle faults (Ramapo fault) and phyllonitic ductile basement rocks of the Ramapo seismic zones, New York and New Jesrey, and their relationship to current seismicity, *in* Manspeizer, W. (ed.). Field studies of New Jersey Geology, New York State Geological Association Guidebook, v. 52, p. 278-311.

Ratcliffe, N.M., 1981, Cortlandt-Beemerville magmatic belt: a probable late Taconian alkali cross trend in the central Appalachians: Geology, v. 9, p. 329-335.

Ratcliffe, N.M., Armstrong, R.L., Mose, D.G., Seneschal, R., Williams, N., and Baiamonte, M.J., 1982, Emplacement history and tectonic significance of the Cortlandt Complex, related plutons, and dike swarms in the Taconide zone of southeastern New York based on K-Ar and Rb-Sr investigations: American Journal of Science, v. 282, p. 358-390.

Sibson, R.H., 1977, Fault rocks and fault mechanics: Jour. Geol. Soc. London, v. 123, p. 191-213.

Simpson, C. and Schmid, S.M., 1983, An evaluation of criteria to deduce the sense of movement in sheared rocks: Geological Society of America Bulletin, v. 94, p. 1281-1293.

Simpson, C., 1985, Deformation of granitic rocks across the brittle-ductile transition: Journal of Structural Geology, v. 7, p. 503-511.

Stauffer, M.R., 1970, Deformation textures in tectonites: Canadian Jour. Earth Sciences, v. 7, p. 498-511.

Tullis, J.A. and Yund, R.A., 1977, Experimental deformation of dry Westerly granite: Journal of Geophysical Research, v. 82, p. 5705-5718.

Tullis, J.A. and Yund, R.A., 1987, Transition from cataclastic flow to dislocation creep of feldspar: Mechanisms and microstructures: Geology, v. 15, p. 591-595.

Volkert, R.A., 1993, Geology of the Middle Proterozoic rocks of the New Jersey Highlands, in (Puffer, J.H., ed.) Geologic Traverse across the Precambrian Rocks of the New Jersey Highlands, Geological Association of New Jersey Field Guide and Proceedings, v. 10, p. 23-55.

Volkert, R.A. and Drake, A.A. Jr., 1999, Geochemistry and stratigraphic relations of Middle Proterozoic rocks of the New Jersey Highlands: U.S. Geological Survey Professional Paper 1565-C, 77 p.

Volkert, R.A., 2001, Geologic setting of Proterozoic Iron, Zinc, and Graphite Deposits, New Jersey Highlands: Society of Economic Geology Guidebook Series, v. 35, p. 59-73.

Volkert, R.A., Aleinikoff, J.N., and Fanning, C.M., 2010, Tectonic, magmatic, and metamorphic history of the New Jersey Highlands: New insights from SHRIMP U-Pb geochronology: Geological Society of America Memoirs, v. 206, p. 307-346.

White, S.H., Burrows, S.E., Carreras, J., Shaw, N.D. and Humphreys, F.J., 1980, On mylonites in ductile shear zones: Journal of Structural Geology, v. 2, p. 175-187.